

High-harmonic electron bunching in the field of a signal wave and the use of this effect in cyclotron masers with frequency multiplication

I. V. Bandurkin and A. V. Savilov*

Institute of Applied Physics, Russian Academy of Sciences, 46 Ulyanov Street, Nizhny Novgorod, 603950, Russian Federation
(Received 11 October 2004; published 20 January 2005)

A method of organizing electron-wave interaction at the multiplied frequency of the signal wave is proposed. This type of electron-wave interaction provides multiplied-frequency electron bunching, which leads to formation of an intense harmonic of the electron current at a selected multiplied frequency of the signal wave. This effect is attractive for the use in klystron-type cyclotron masers with frequency multiplication as a way to increase the output frequency and improve the selectivity.

DOI: 10.1103/PhysRevSTAB.8.010702

PACS numbers: 84.40.Ik, 84.40.Fe

I. INTRODUCTION

Cyclotron resonance masers (CRMs) with frequency multiplication (conversion) are considered as attractive sources of high-power coherent radiation in the short-millimeter and submillimeter ranges of wavelengths. Their principle of operation is based on selective spontaneous phase-locked emission from prebunched electron beams at higher harmonics [1–3]. A principal scheme of the klystron-type variant of such a device is shown in Fig. 1(a). In the first cavity, electrons are influenced by the bunching force, $F(\omega)$ at the frequency of the input rf wave ω ; this results in electron bunching at frequency ω and its higher harmonics. In the simplest case of the electron-wave interaction at the fundamental harmonic, a single bunching center appears on the Larmor circle, which is initially filled with electrons uniformly. Before entering the second cavity, the electron beam contains electron-current harmonics ρ_n at frequencies $n\omega$. Therefore, in this cavity it can radiate at one of these harmonics, $N\omega$; evidently, the number of the cyclotron harmonic of the electron-wave interaction coincides with the number N of the “operating” electron-current harmonic [1].

This paper is devoted to improvement of the operation of the first section [Fig. 1(b)]. It is shown that there exists a possibility to realize the frequency multiplication already in the bunching section. This is the case when the signal wave influences the electrons with a bunching force at the multiplied frequency $F(q\omega)$, and, therefore, the prebunched electron beam contains only higher electron-current harmonics ρ_{qn} and can radiate in the second cavity at frequencies $qn\omega$. A special case of the proposed scheme, when the interaction between electrons and the signal wave occurs at the doubled frequency $q = 2$ has been studied in Ref. [4]; in this case the prebunched

electron beam contains only even electron-current harmonics ρ_{2n} , and, correspondingly, the frequency multiplication factor is $N = 2n$.

The advantages of this scheme are evident. In the case of ideal multiplication, the absence of electron-current harmonics with numbers, which are different from qn (including the most dangerous fundamental harmonic), gives a chance to improve the selectivity significantly. In addition, since values of ρ_{qn} in the scheme shown in Fig. 1(b) are as large as values of ρ_n in the scheme shown in Fig. 1(a), the possibility to provide a better electron bunching at higher harmonics appears.

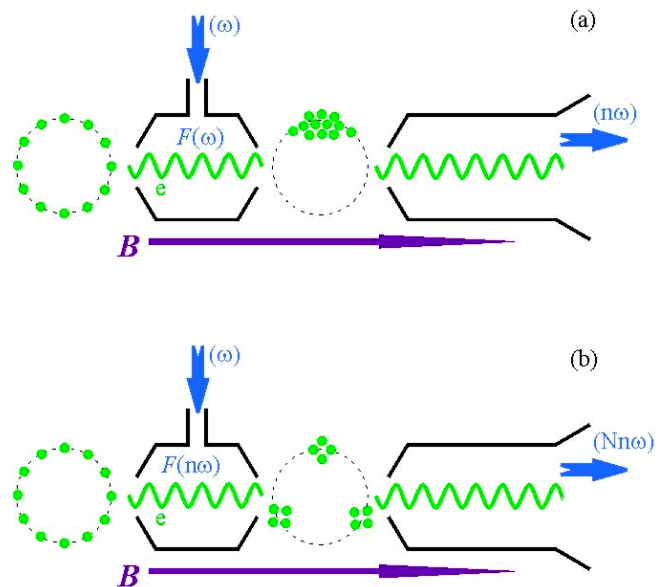


FIG. 1. (Color) Principal schematic of a CRM with frequency multiplication and electron bunching in the case of the fundamental-cyclotron-harmonic interaction in the bunching section. The cases of the electron-wave interaction inside the bunching section at the frequency of the input signal (a) and at the multiplied (namely, triple) frequency (b).

*Email address: savilov@appl.sci-nnov.ru
Telephone: +7-8312-164818
Fax: +7-8312-160616

II. ELECTRON-WAVE INTERACTION WITH FREQUENCY MULTIPLICATION

We consider the motion of electrons in the field of a rf wave under the resonance condition:

$$\omega \approx hv_z + \Omega. \quad (1)$$

Here ω and h are the frequency and the longitudinal wave number of the rf wave, v_z is the axial electron velocity, and Ω is the frequency of electron oscillations (the relativistic cyclotron frequency in CRMs). The mechanism of providing electron bunching at the multiplied frequency of the wave can be described on the basis of asymptotic equations of electron motion, which are valid for a wide class of electron devices [5,6],

$$\frac{dw}{dz} = a \operatorname{Re}\{\chi e^{i\phi}\}, \quad \frac{d\phi}{dz} = \nu w - \Delta. \quad (2)$$

Here w is the change of electron energy, z is the axial coordinate, a is the rf wave amplitude, $\phi = \omega t - hz - \int \Omega dt$ is the electron phase with respect to the wave, χ and ν are factors of electron-wave coupling and of the electron bunching, respectively, and $\Delta = -(\omega - hv_z - \Omega)/v_z$ is the mismatch of the electron-wave resonance. At the beginning, $z = 0$, initial phases of particles of an electron beam are distributed uniformly within the interval $0 \leq \phi_0 < 2\pi$.

Let us consider the situation when the coupling factor is a periodic function of the coordinate, $\chi(z) = \chi(z + L_\chi)$, so that it can be represented as a Fourier expansion, $\chi(z) = \sum \chi_m e^{imhz}$, where $\hbar = 2\pi/L_\chi$. If period L_χ is much smaller than the characteristic length of the electron-wave coupling, $L_\chi \ll (a\chi_{\max}\nu)^{-1/2}$, where χ_{\max} is the maximum of $\chi(z)$, such a profiling causes small perturbations of the electron motion. This allows splitting w and ϕ

into slow (averaged) and fast (oscillating) components [7]:

$$w = W + w_\sim, \quad \phi = \Phi + \phi_\sim \quad (\phi_\sim \ll \pi). \quad (3)$$

Representing the fast phase in the form $\phi_\sim = \sum_{m \neq 0} \phi_m e^{imhz}$ and expanding it into Taylor series, $\exp(i\phi_\sim) = 1 + i\phi_\sim + \frac{(i\phi_\sim)^2}{2} + \dots$, one can conclude the following equations for slow components of energy and phase:

$$\frac{dW}{dz} = a \operatorname{Re}\left\{e^{i\Phi}\left(\chi_0 + i \sum_{s \neq 0} \phi_s \chi_{-s} - \sum_{p,q \neq 0} \phi_p \phi_q \chi_{-p-q} + \dots\right)\right\}, \quad (4)$$

$$\frac{d\Phi}{dz} = \nu W - \Delta,$$

and the recurrent expression for spatial harmonics of ϕ_\sim :

$$\begin{aligned} \phi_m = & -\frac{\nu a}{2m^2 \hbar^2} e^{i\Phi} \left(\chi_m + i \sum_{s \neq 0} \phi_s \chi_{m-s} \right. \\ & \left. - \sum_{p,q \neq 0} \phi_p \phi_q \chi_{m-p-q} + \dots \right) \\ & - \frac{\nu a}{2m^2 \hbar^2} e^{-i\Phi} \left(\chi_{-m}^* - i \sum_{s \neq 0} \phi_s^* \chi_{-m-s}^* \right. \\ & \left. - \sum_{p,q \neq 0} \phi_p^* \phi_q^* \chi_{-m-p-q}^* + \dots \right). \end{aligned} \quad (5)$$

For various factors of multiplication m , coefficients ϕ_m and, hence, the right-hand part of the equation for the electron energy (4) can be found from (5) by the method of successive approximations, $\phi_m = \phi_m^{(0)} + \phi_m^{(1)} + \phi_m^{(2)} + \dots$, with small parameter $\mu = \frac{\nu a \chi}{\hbar^2} \ll 1$:

$$\begin{aligned} \phi_m^{(0)} &= 0, \quad \phi_m^{(1)} = -\frac{\nu a}{2m^2 \hbar^2} (\chi_m e^{i\Phi} + \chi_{-m}^* e^{-i\Phi}), \\ \phi_m^{(2)} &= i \frac{\nu^2 a^2}{4m^2 \hbar^4} \sum_{s \neq 0} \frac{\chi_s \chi_{m-s} e^{2i\Phi} - \chi_s^* \chi_{-m-s}^* e^{-2i\Phi} + \chi_{-s}^* \chi_{m-s} - \chi_{-s} \chi_{-m-s}^*}{s^2}, \end{aligned} \quad (6)$$

and so on. Since the order of smallness of ϕ_m^k appears to be not greater than μ^k , such a procedure is correct. Substitution of (6) into (4) yields

$$\frac{dW}{dz} \approx \operatorname{Re}\{S_1^+ e^{i\Phi} + S_1^- e^{-i\Phi}\} + \operatorname{Im}\{S_2 e^{2i\Phi}\} + \operatorname{Re}\{S_3 e^{3i\Phi}\} + \dots, \quad (7)$$

where

$$\begin{aligned} S_1^+ &\approx a \left(\chi_0 - \frac{\nu^2 a^2}{4\hbar^4} \sum_{s,p \neq 0} \frac{3\chi_s \chi_p^* \chi_{p-s} - \chi_s \chi_p \chi_{s-p}^*}{s^2 p^2} \right), & S_1^- &\approx a \left(\frac{\nu^2 a^2}{4\hbar^4} \sum_{s,p \neq 0} \frac{\chi_s \chi_p^* \chi_{s-p}^* - \chi_s^* \chi_p \chi_{s+p}}{s^2 p^2} \right), \\ S_2 &\approx a \left(\frac{\nu a}{2\hbar^2} \sum_{s \neq 0} \frac{\chi_s \chi_{-s}}{s^2} \right), & S_3 &\approx -a \left(\frac{\nu^2 a^2}{2\hbar^4} \sum_{s,p \neq 0} \frac{\chi_s \chi_p \chi_{-s-p}}{s^2 p^2} \right). \end{aligned} \quad (8)$$

In the right-hand part of Eq. (7), the first term describes the electron-wave interaction at the frequency of the signal wave; this interaction is weak when $\chi_0 = 0$. The second term ($\sim S_2 e^{2i\Phi}$) is responsible for the interaction at the doubled frequency, and the next term ($\sim S_3 e^{3i\Phi}$) describes the bunching force at the triple frequency. Evidently, the right-hand part

of Eq. (7) includes also the higher-order terms ($\sim S_n e^{ni\Phi}$), which correspond to electron-wave interaction at the frequencies $n\omega$.

As an example, let us consider the following simplest case:

$$\chi(z) = e^{i\hbar z} + e^{-i\hbar z} = 2i \sin(\hbar z),$$

when $\chi_{\pm 1} = 1$, whereas all other coefficients of the Fourier expansion of $\chi(z)$ are equal to zero. In this case, the only nonzero factor in (8) is $S_2 = \frac{\nu^2 a^2}{\hbar^2}$ and, therefore, the signal wave interacts with electrons at the doubled frequency. In the case of a more complicated profile of $\chi(z)$,

$$\chi(z) = e^{i\hbar z} + e^{-2i\hbar z},$$

when $\chi_1 = \chi_{-2} = 1$, the only nonzero factor is $S_3 = \frac{\nu^2 a^3}{8\hbar^4}$, which corresponds to the interaction at the triple frequency. In general, a profile having the following form,

$$\chi(z) = A_1 e^{i\hbar z} + A_2 e^{-(n-1)i\hbar z},$$

provides electron-wave interaction at the frequency $n\omega$.

III. PONDEROMOTIVE-FORCE INTERPRETATION

In the case of the frequency doubling, $n = 2$, this effect can be explained in terms of the averaged ponderomotive force (so-called Miller force [8]). As an example, we consider electron-wave interaction in a CRM at the exact ($\Delta = 0$) fundamental-harmonic resonance, and study the case of the klystron-type dependence of the coupling coefficient on the coordinate, $\chi(z) = \hat{\chi} L_\chi [\delta(z) - \delta(z - L_\chi/2)]$ within the interval $0 \leq z < L_\chi$ [here $\delta(z)$ is the delta function]. The electron bunching under the effect of the force $F = a\chi \cos\phi$ is illustrated in Fig. 2. Let us compare the motion of two electrons with initial phases $\pm\phi_0$. At the beginning, $z = 0$, these electrons get the same positive push from the bunching force,

$$\left. \frac{d\phi_\pm}{dz} \right|_{z=+0} - \left. \frac{d\phi_\pm}{dz} \right|_{z=-0} = av\hat{\chi}L_\chi \cos\phi_0,$$

and within the interval $0 < z < L_\chi/2$ both of them go up: $\phi_\pm(z) = \pm\phi_0 + av\hat{\chi}L_\chi z \cos\phi_0$. It is important that the upper electron ($+\phi_0$) shifts toward the point of zero bunching force, $\phi = \pi/2$, whereas the lower one ($-\phi_0$) moves toward the maximum of $F(\phi)$, $\phi = 0$ [Fig. 2(a)]. Then, at the point $z = L_\chi/2$ both the electrons get a negative push from the bunching force,

$$\left. \frac{d\phi_\pm}{dz} \right|_{z=+L_\chi/2} - \left. \frac{d\phi_\pm}{dz} \right|_{z=-L_\chi/2} = -av\hat{\chi}L_\chi \cos\phi_\pm,$$

so that the full effect of two pushes is expressed in the following form:

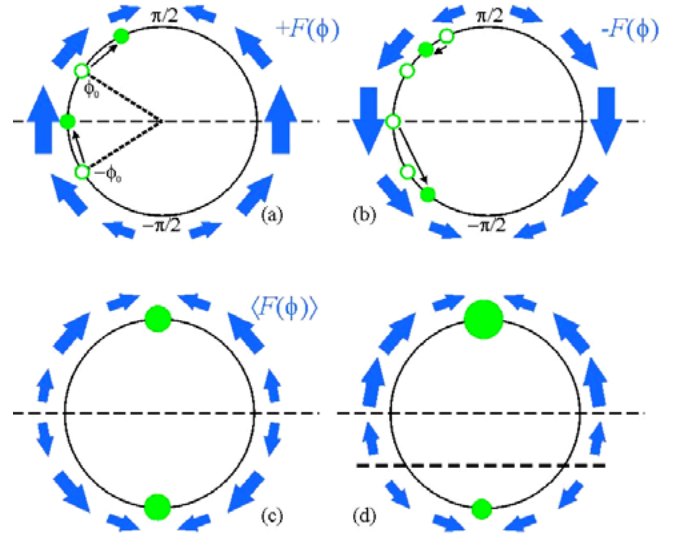


FIG. 2. (Color) Electron bunching in the case of the klystron-type profile of the electron-wave coupling factor: motion of particles over the Larmor orbit after the first, positive, push (a) and the second, negative, push (b) from the input wave, symmetrical averaged bunching force (c), and nonsymmetrical electron bunching (d).

$$\begin{aligned} \left. \frac{d\phi_\pm}{dz} \right|_{z=+L_\chi/2} &= av\hat{\chi}L_\chi \cos\phi_0 - av\hat{\chi}L_\chi \cos\phi_\pm \\ &\approx \pm \frac{(av\hat{\chi}L_\chi)^2}{4} L_\chi \sin 2\phi_0. \end{aligned}$$

Since the displacement of the electrons with respect to the maximum of $F(\phi)$ is opposite, the absolute value of the second push is smaller (as compared to first one) for the upper electron, and it is greater for the lower one [Fig. 2(b)]. Thus, the averaged force is positive for the upper particle and negative for the lower one. Hence, symmetrical electron bunching with two centers, which are $\phi = \pi/2$ for upper ($0 < \phi_0 < \pi$) electrons and $\phi = -\pi/2$ for lower ($-\pi < \phi_0 < 0$) ones, occurs [Fig. 2(c)]. The existence of two bunching centers during the process of the electron-wave interaction at the fundamental cyclotron resonance corresponds to doubling of the frequency of electron bunching.

Although the averaged bunching force is symmetrical, the klystron-type approach predicts the nonsymmetrical character of the nonaveraged electron motion [Fig. 2(d)]:

$$\begin{aligned} \phi_\pm(L) &= \pm\phi_0 + av\hat{\chi}L_\chi \frac{L_\chi}{2} \cos\phi_0 \\ &\quad \pm \frac{(av\hat{\chi}L_\chi)^2}{8} L_\chi^2 \sin 2\phi_0. \end{aligned} \quad (9)$$

All upper electrons shift to the bunching center $\phi = \pi/2$, but at the same time part of the lower ones move toward this point too. The reason for such nonsymmetry is the existence of the preferential direction, which is the direc-

tion of the first push, as well as the inertia of particles. Formally, the nonsymmetry is associated with the second term of expression (9), which corresponds to the electron motion between the first and the second pushes. This effect makes worse the electron bunching at even harmonics and spoils the selectivity due to the appearance of odd harmonics (especially the fundamental one).

An obvious way to avoid the nonsymmetry of the electron bunching is to decrease the effect of the first push. Namely, smooth entrance of electrons into the interaction region should be used; this can be provided by creating a smoothly increasing profile of the rf amplitude (or the coupling coefficient) at the beginning of the interaction region. This is illustrated by calculations of (2) using sinusoidal profiling of the coupling coefficient, $\chi(z) = \sin(2\pi z/2.5)$, in the cases of uniform rf wave amplitude, $a = 1$, and a tapered amplitude,

$$a(z) = \begin{cases} z/15, & 0 \leq z \leq 15, \\ 1, & z > 15. \end{cases}$$

In these calculations, the spread in electron velocity is modeled by uniform distribution of the mismatch within the interval $-0.1 \leq \Delta \leq 0.1$. Figure 3 illustrates evolutions of the first and second harmonics of the electron current, $\rho_{1,2}$. In the case of the uniform rf wave amplitude, both electron-current harmonics grow together up to the value of about 0.4 [Fig. 3(a)], whereas the input profiling of $a(z)$ leads to improved electron bunching at the second harmonic, $|\rho_2| \approx 0.6$, and to almost total disappearance of the first harmonic, $|\rho_1| < 0.05$ [Fig. 3(b)].

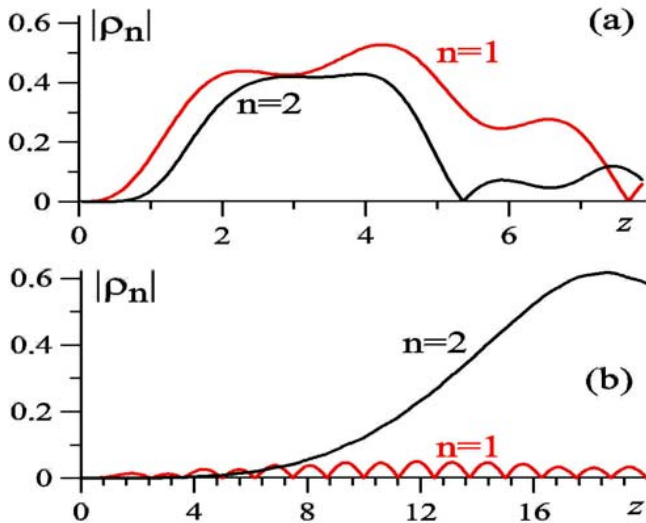


FIG. 3. (Color) Results of simulations of universal asymptotic equations (2) in the cases of the uniform wave amplitude (a) and of a smooth entrance of electrons into the interaction region (b). First and second harmonics of the electron current versus the axial position.

IV. TWO-WAVE INTERPRETATION

Let us consider the case when the electron-wave coupling factor has the following profile,

$$\chi(z) = A_1 \exp(im_1 \hbar z) + A_2 \exp(-im_2 \hbar z),$$

and assume that the integer numbers m_1 and m_2 are coprime. Evidently, in this case in the right-hand part of Eq. (7) the averaged bunching force at the frequency $n\omega$, $\text{Im}\{S_n e^{in\phi}\}$, is determined by a term like this:

$$S_n \sim \sum_p A_1^p A_2^{n-p} \overline{\exp[i(p m_1 - n m_2 + p m_2)z]}^z.$$

This sum can include one nonzero item, provided that item's number p satisfies the following condition:

$$p(m_1 + m_2) = n m_2.$$

Evidently, this is possible only if $m_1 + m_2 = n$ (and the number of the nonzero item is $p = m_2$).

Thus, the chosen profile of the coupling factor should provide electron-wave interaction at the frequency $(m_1 + m_2)\omega$. On the other hand, in this case the motion equations (2) take the following form:

$$\begin{aligned} \frac{dw}{dz} &= \text{Re}\{a_1 \exp(i\phi_1) + a_2 \exp(i\phi_2)\}, \\ \frac{d\phi_1}{dz} &= \nu w + m_1 \hbar, \quad \frac{d\phi_2}{dz} = \nu w - m_2 \hbar, \end{aligned} \quad (10)$$

where $a_k = aA_k$. These equations correspond to the case of interaction of electrons with two waves, which have cyclotron-resonance mismatches $\Delta_1 = -m_1 \hbar$ and $\Delta_2 = m_2 \hbar$, so that

$$m_2 \Delta_1 + m_1 \Delta_2 = 0.$$

Note that the requirement for smallness of the period $L_\chi = 2\pi/\hbar$ of the profile of the coupling factor means that the waves should be far enough from the cyclotron resonance (1).

In terms of parameters of two waves with frequencies ω_1, ω_2 and longitudinal wave numbers h_1, h_2 , condition $m_2 \Delta_1 + m_1 \Delta_2 = 0$ takes the following form:

$$m_2(\omega_1 - h_1 \nu_z - \Omega) + m_1(\omega_2 - h_2 \nu_z - \Omega) = 0.$$

This can be rewritten as the following condition of the ‘‘average’’ two-wave resonance:

$$\frac{m_2 \omega_1 + m_1 \omega_2 - (m_2 h_1 + m_1 h_2) \nu_z}{m_1 + m_2} = \Omega. \quad (11)$$

If this condition is fulfilled, then there exists a slow combination phase, $m_2 \phi_1 + m_1 \phi_2$, whereas the cyclotron phases of electrons with respect to the waves, $\phi_{1,2} = \omega_{1,2} t - h_{1,2} z - \int \Omega dt$, are relatively fast. The averaged ponderomotive force has the following dependence on the slow phase:

$$\langle F \rangle \propto a_1^{m_2} a_2^{m_1} \exp[i(m_2 \phi_1 + m_1 \phi_2)]; \quad (12)$$

therefore, the electron bunching at the frequency $m_2 \omega_1 + m_1 \omega_2$ is to be provided. In the case of $\omega_1 = \omega_2 = \omega$, this means multiplication of the input frequency with factor $n = m_1 + m_2$.

V. ELECTRON BUNCHING AT HIGHER HARMONICS IN BRAGG CAVITIES

Thus, there are two equivalent methods to provide electron bunching at a multiplied frequency of the signal wave. The first one is the use of a signal wave, which is close to the cyclotron resonance with electrons, along with a periodical profiling of the electron-wave coupling factor $\chi(z)$. The second way is the use of two waves, which are relatively far from the cyclotron resonance (1) but close to the two-wave averaged resonance (11).

Apparently, the most attractive variant is the realization of the second method for the case of two counterpropagating traveling waves with equal frequencies $\omega_1 = \omega_2 = \omega$ and rational relation of longitudinal wave numbers $h_1/h_2 = -m_1/m_2$, when condition (11) is reduced to the following simple form [Fig. 4(a)]:

$$\omega = \Omega. \quad (13)$$

Such a scheme can be realized in a Bragg cavity [Fig. 4(b)]

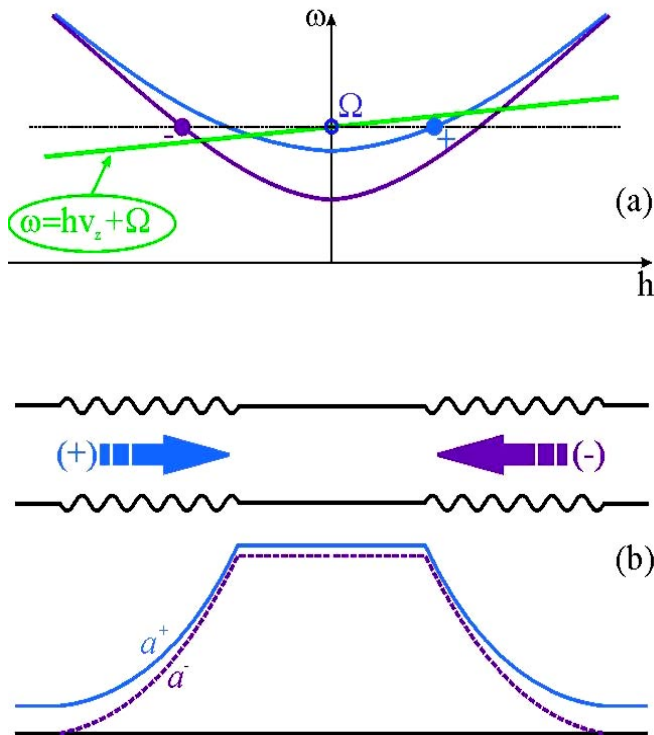


FIG. 4. (Color) Dispersion diagram for the case of the averaged two-wave resonance (a) and longitudinal structure of forward and backward waves inside the microwave system of the bunching section (b).

[9], when a forward-propagating wave with its longitudinal wave number h_1 , which is put in the resonator by the input mirror, transforms inside the output Bragg reflector to the backward-propagating wave with longitudinal wave number $h_2 = -h_1 m_2 / m_1$ and then back again to the initial wave inside the input reflector. The following relation between the wave numbers should be observed for this transformation:

$$h_2 = h_1 - \frac{2\pi}{d},$$

where d is the period of the Bragg structure. The longitudinal distribution of the forward and backward waves inside the cavity is illustrated in Fig. 4(b). If the input and output mirrors are equal, and the frequency of the waves coincides with the eigenfrequency of the cavity, then reflection of the input wave from the resonator is absent and the forward wave has the same amplitudes both at the input and output.

Advantages of this scheme are the simplicity of its realization, as well as the unique character of the electron-wave interaction. Indeed, the frequency ω can be far from the cutoff. However, resonance condition (13) and the operating phase of the resonant ponderomotive force (12),

$$m_2 \phi_1 + m_1 \phi_2 = n \left(\omega t - \int \Omega dt \right), \quad n = m_1 + m_2,$$

have the gyrotronlike character; namely, they do not include the longitudinal electron velocity. Therefore, the bunching process has weak sensitivity to the velocity spread. One more advantage is the simplicity of providing a smooth entrance of electrons into the interaction region (as well as a smooth output), which is needed to achieve ideal frequency multiplication (see the end of Sec. II). Mutual scattering of the forward and backward waves inside the Bragg reflector provides smoothly increasing/decreasing profiles of the rf amplitudes [Fig. 4(b)], which is equivalent to smooth profiling of the coupling factor.

Numerical simulations based on the nonaveraged equations of electron motion in a rf field with a fixed spatial structure confirm the possibility to provide electron bunching at a multiplied frequency. As an example, we examine the case of a beam of electrons moving in the longitudinal uniform magnetic field and encircling the axis of a Bragg cavity with a circular cross section. Electrons interact with a superposition of two counterpropagating waves, which are the waveguide modes $TE_{1,s}$ and $TE_{1,p}$ having the free-space wavelength $\lambda = 8$ mm and being far from the cutoff. The uniform magnetic field corresponds to the exact resonance condition (13).

In numerical simulations we succeeded in achieving electron bunching at up to the fourth harmonic of the signal wave frequency. The results of these simulations are illustrated in Table I. It should be noted that for $m_1 = m_2 = 1$

TABLE I. Parameters and results of numerical simulations.

Frequency multiplication factor n	2	3	4
Electron energy	20 keV	20 keV	40 keV
Averaged electron pitch factor	1	1	1.4
Total length of the Bragg sections	8.5 cm	14.9 cm	20 cm
Length of regular waveguide section	6 cm	6.9 cm	10.9 cm
Waveguide modes (forward/backward waves)	TE _{1,1} /TE _{1,1}	TE _{1,2} /TE _{1,3}	TE _{1,2} /TE _{1,3}
Forward-wave power at the input/middle of the cavity	0.1/15 kW	0.5/70 kW	4.5/40 kW
Electron-current harmonic ρ_n for the ideal beam	0.6	0.6	0.6
Electron-current harmonic ρ_n for 10%/15% velocity spread	0.6/0.6	0.6/0.5	0.4/0.3
Ratio ρ_n/ρ_1 at the maximum of ρ_n for 15% spread	>20	>10	~2

(which corresponds to frequency doubling, $n = 2$) the waveguide radius can be chosen optionally, because in this case both the forward and the backward waves are formed by the same mode TE_{1,1} (in simulations the case of $v_{gr} = 0.8c$ is chosen). At the same time, for different m_1 and m_2 (which corresponds to the bunching at harmonic $n = m_1 + m_2 > 2$), the waveguide radius R is determined from the condition

$$h_1^2 + \frac{\xi_s^2}{R^2} = h_2^2 + \frac{\xi_p^2}{R^2} = \frac{\omega^2}{c^2},$$

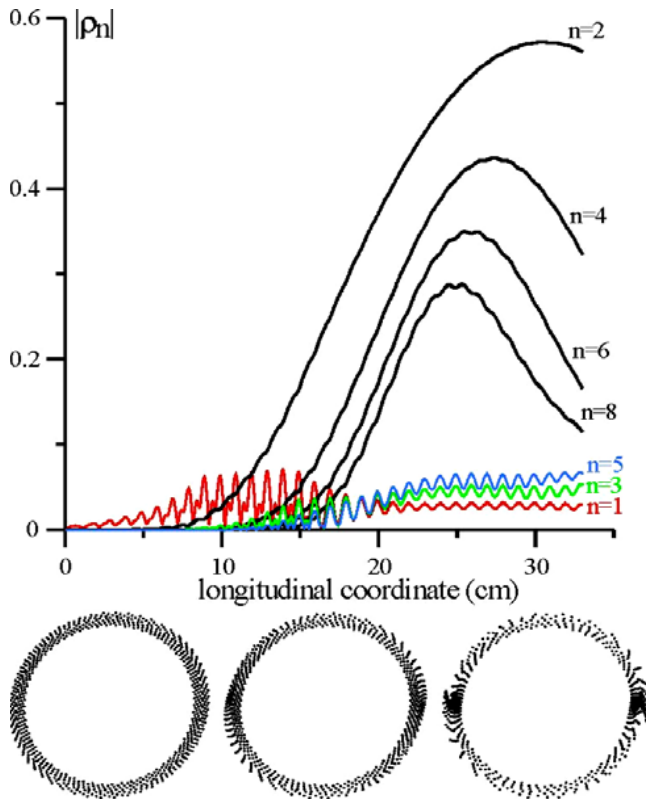


FIG. 5. (Color) Frequency doubling: operating (black curves) and spurious (color curves) harmonics of the electron current ρ_n versus the longitudinal coordinate and distribution of electrons over their gyrophases and Larmor radii for the case of 15% velocity spread.

where $\xi_{s,p}$ are the corresponding zeroes of the first-order Bessel derivative.

Let us notice that although the resonance condition (13) has a gyrotronlike character (it does not include the electron velocity), at great frequency multiplication factors n a significant sensitivity to the spread in electron velocity occurs. The evident reason is a strengthening of the dependence of the bunching force (12) on the velocity with the

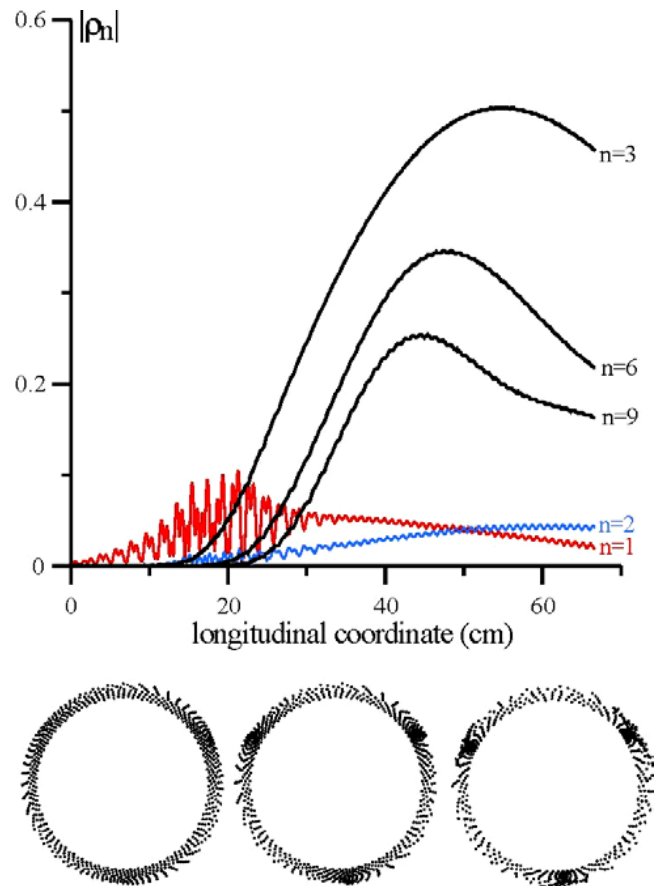


FIG. 6. (Color) Frequency tripling: operating (black curves) and spurious (color curves) harmonics of the electron current ρ_n versus the longitudinal coordinate and distribution of electrons over their gyrophases and Larmor radii for the case of 15% velocity spread.

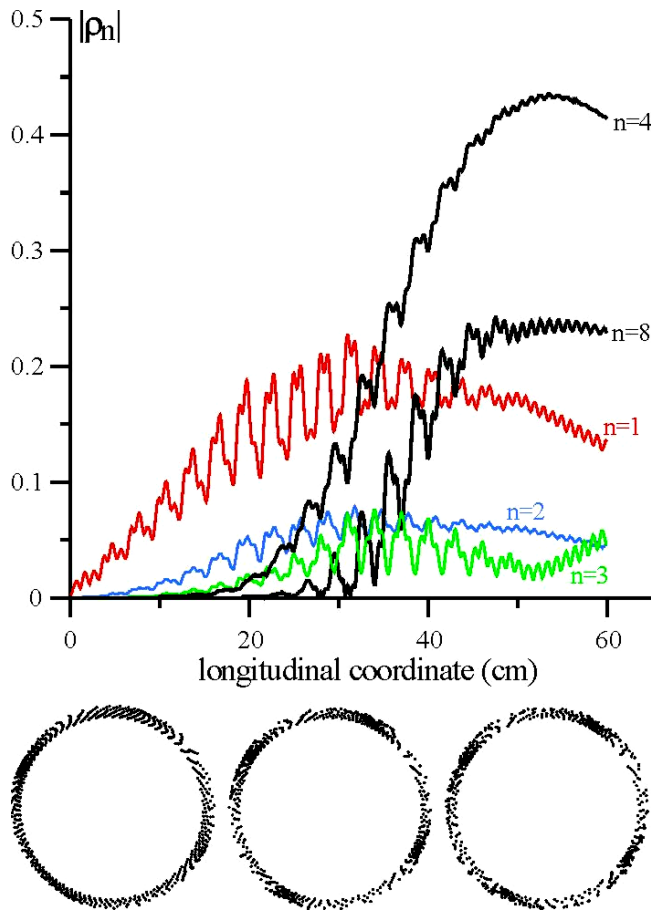


FIG. 7. (Color) Frequency quadrupling: operating (black curves) and spurious (color curves) harmonics of the electron current versus the longitudinal coordinate ρ_n distribution of electrons over their gyrophases and Larmor radii for the case of 10% velocity spread.

increase of n . Actually, the coupling factor for each wave in Eq. (10) is proportional to the pitch factor: $a_{1,2} \propto v_{\perp}/v_{\parallel}$. Since $S_n \propto \chi^n$, the bunching force at the n th harmonic is proportional to the n th degree of pitch factor, $F(n\omega) \propto (v_{\perp}/v_{\parallel})^n$.

Figures 5–7 illustrate the dependence of electron-current harmonics on the longitudinal coordinate, as well as the form of electron bunches on the Larmor circle. Simulations demonstrate electron bunching at a multiplied frequency with very high efficiency for an ideal beam and, at the same time, gradually increasing influence of the velocity spread upon the bunching quality with enhancement of the multiplication factor n . In all cases, after the bunching section the electron beam contains intense current harmonics divisible by n ($|\rho_n| \approx 0.6$ without spread), whereas the values of other harmonics are considerably small. It is also important that the bunching leads to a very small additional spread in electron energy (for instance, the

averaged change in electron energy does not exceed 0.5% in the case of frequency doubling). This means that bunching process can be quite correctly described by simple asymptotic equations (10).

VI. CONCLUSION

It is shown that there exists a possibility to organize electron-wave interaction at the multiplied frequency of the signal wave, and, therefore, to provide the multiplied-frequency electron bunching. This leads to the appearance of only high-number harmonics of the current in the electron beam, whereas values of undesired low harmonics (including the fundamental one) stay considerably small. This effect seems to be attractive for use in the bunching sections of klystron-type electron masers (including CRMs) with frequency multiplication as a way to increase the output frequency and to improve selectivity. Such an interaction takes place if a single wave is in the cyclotron resonance with electrons and a special periodical profiling of the electron-wave coupling factor is provided. This is analogous to the case of electron bunching in the field of two waves, which are close to the special two-wave resonance. Apparently, the most attractive variant of such a realization of the effect is the use of two counterpropagating waves, which form a periodical rf structure inside the cavity.

ACKNOWLEDGMENTS

The authors are grateful to Professor V.L. Bratman for useful discussions. This work is supported by the Russian Foundation for Basic Research, Projects No. 02-02-17205 and No. 04-02-17118, as well as by the Russian Science Support Foundation.

- [1] J.L. Hirshfield, Phys. Rev. A **44**, 6845 (1991).
- [2] J.L. Hirshfield, C. Wang, and A.K. Ganguly, IEEE Trans. Plasma Sci. **24**, 825 (1996).
- [3] H. Guo, S.H. Chen, V.L. Granatstein, J. Rogers, G.S. Nusinovich, M. T. Walter, B. Levish, and W. J. Chen, Phys. Rev. Lett. **79**, 515 (1997).
- [4] A. V. Savilov, IEEE Trans. Plasma Sci. **32**, 1147 (2004).
- [5] W.B. Colson, W.H. Louisell, J.F. Lam, and C.D. Cantrell, J. Opt. Soc. Am. **68**, 1620 (1978).
- [6] V.L. Bratman, N.S. Ginzburg, and M.I. Petelin, Opt. Commun. **30**, 409 (1979).
- [7] A. V. Savilov, Nucl. Instrum. Methods Phys. Res., Sect. A **372**, 539 (1996).
- [8] M. A. Miller, Izv. Vuzov Radiofizika **1**, 110 (1958) (in Russian).
- [9] V.L. Bratman, G.G. Denisov, N.S. Ginzburg, and M.I. Petelin, IEEE J. Quantum Electron. **19**, 282 (1983).